A Modular Approach to Bio-Based Poly(enol ether)s with Tunable Thermal Properties and Degradability

Tarek Ibrahim, Hao Sun*

Department of Chemistry and Chemical & Biomedical Engineering, Tagliatela College of Engineering, University of New Haven, West Haven, CT, USA, 06516

ABSTRACT: Biomass-derived polymer materials are emerging as sustainable and low carbon-footprint alternatives to the current petroleum-based commodity plastics. In the past decade, ring-opening metathesis polymerization (ROMP) technique has been widely used for the polymerization of cyclic olefin monomers derived from bio-renewable resources, giving rise to a diverse set of bio-based polymer materials. However, most of synthetic bio-based polymers made by ROMP are non-degradable because of their all-carbon backbones. Herein, we present a modular synthetic strategy to acid-degradable poly(enol ether)s via ring-opening metathesis copolymerization of bio-renewable oxanorbornenes and 3,4-dihydropyran (DHP). ^{1}H NMR analysis reveals that the percentage of DHP units in the resulting copolymers gradually increases as the feed ratio of DHP to oxanorbornene increases. The composition of copolymers plays a pivotal role in governing their thermal properties. Thermogravimetric analysis shows that an increasing percentage of DHP results in a decrease in the decomposition temperatures, suggesting that the incorporation of enol ether groups in the polymer backbone reduces the thermal stability of copolymers. Moreover, a wide range of glass transition temperatures (16-165 °C) can be achieved by tuning the copolymer composition and oxanorbornene structure. Critically, all the poly(enol ether)s developed in this study are degradable under mildly acidic conditions. A higher incorporation of DHP in the copolymer leads to an enhanced degradability, as evidenced by smaller final degradation products. Altogether, this study provides a facile approach for synthesizing bio-renewable and degradable polymer materials with highly tunable thermal properties desired for their potential industrial applications.

KEYWORDS: degradable polymers, sustainable materials, poly(enol ether)s, biomass-derived, 3,4-dihydropyran

1. Introduction

Synthetic polymers have infiltrated almost every aspect of our modern life, reaching a staggering production level of more than 400 million metric tons in 2022.[1] They are ubiquitous in a broad spectrum of applications, spanning from industrial materials (e.g., packaging, coating, and adhesives) to high value-added products such as drug delivery systems and organic batteries.[2-3] Nevertheless, the vast majority (> 99%) of commodity polymers are prepared from petroleum-based feedstocks, which are finite and nonrenewable.[4] Moreover, traditional petroleum-based polymers generate high greenhouse gas emissions stemming from their production and conversion from fossil fuels.[5] In view of this, it is imperative to find a sustainable and low carbon-footprint resource to replace petroleum for polymer production in the near future.

In pursuit of next-generation polymers with carbon neutrality and reduced dependence on petroleum supply, researchers have recently turned their attention to biomass feedstocks, especially those based on plants.[6] The global land-based biomass production by agriculture and forestry is estimated at 11.9 billion metric tons per year, making it an abundant and renewable resource for energy and chemicals.[7] In addition, plants are able to capture carbon dioxide through photosynthesis while growing, offsetting the carbon emissions of bio-based polymers during their manufacturing and combustion after their usage life.[8]

The recent applications of controlled polymerization techniques in biomass resources have unlocked the access to a library of well-defined biomass-derived polymers with novel structures, predetermined molecular weights, and desired properties.[6, 9] In this emerging direction, biomass-derived small molecules are incorporated with a polymerizable functionality that allows them to polymerize via a specific controlled polymerization mechanism such as reversible-deactivation radical polymerization,[10-13] cationic ring-opening polymerization,[14-17] and ring-opening metathesis polymerization (ROMP).[18-30] Among those polymerization techniques, ROMP has received an increasing interest in producing bio-based polymers due to its excellent functional group compatibility and high tolerance to air and water.[31] To date, a variety of biomass-derived feedstocks, including apopinene,[18] δ-pinene,[20-21] terpenoid,[19] rosin,[22] lignin,[23] fatty acid,[24] levoglucosenone,[25, 29] sinapic acids,[27] itaconic anhydride,[26] vanillin,[28] and d-glucose,[30] have been transformed into synthetic polymers by ROMP method. Despite the significant progress in ROMP synthesis of biomass-derived polymers, most of those polymers have non-degradable all-carbon backbones, which raise concerns in their long-term environmental impacts.

Cyclic enol ethers such as five-membered 2,3-dihydrofuran (DHF) have recently emerged as a new class of bio-derived and commercially available monomers for ROMP.[32] In particular, ring-opening metathesis copolymerization of 2,3-dihydrofuran and different comonomers have given rise to a diverse set of poly(enol ether)s that are hydrolysable under acidic conditions.[33-38] 3,4-dihydropyran (DHP) can be produced by dehydration reaction of bioderived tetrahydrofurfuryl alcohol.[39] Compared to the popular 2,3-dihydrofuran, the six-membered DHP remains rarely explored in ROMP synthesis mainly due to its negligible ring strain energy (RSE) that render the polymerization

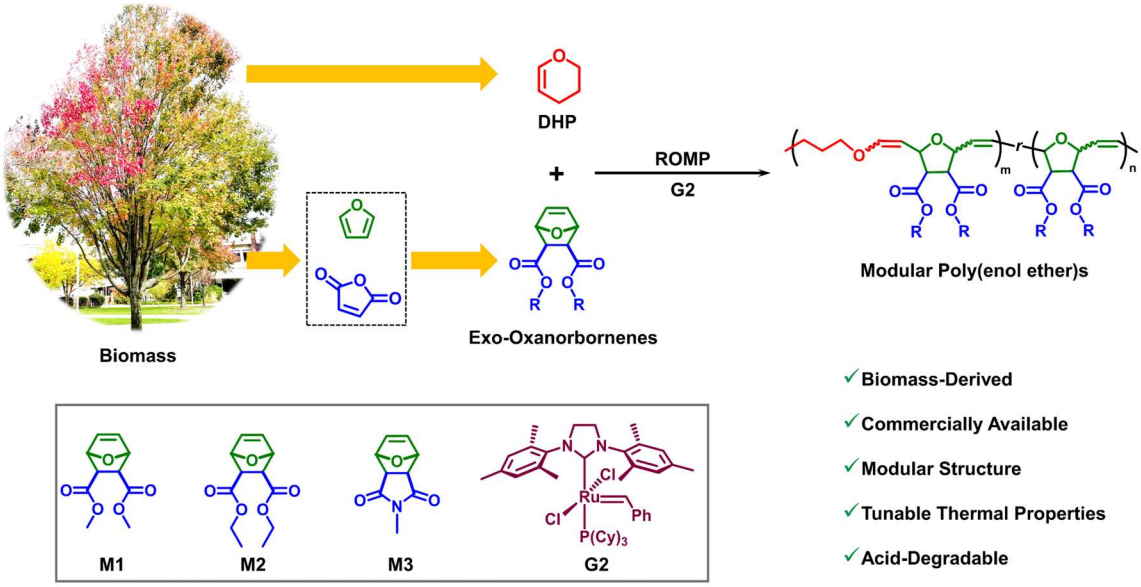

Figure 1. Modular synthesis of biomass-derived and acid-degradable poly(enol ether)s via ring-opening metathesis copolymerization of 3,4-dihydropyran (DHP) and exo-oxanorbornenes (M1-M3).

Table 1. ROMP copolymers of DHP and oxanorbornenes (ONB)

Polymer	ONB	$[ONB]_0$:$[DHP]_0$:$[G2]_0$	Polymerization Time (h)	Monomer Conversion (%)[a]	Comonomer Incorporation (ONB: DHP)[b]	$M_{n,SEC}$ (kDa)[c]	$Đ$[c]	$T_{d,5\%}$ (°C)	T_g (°C)
P1a	**M1**	60:3000:1	3	>95	100:74	18.7	1.5	302.2	36.9
P1b	**M1**	60:1500:1	3	>95	100:63	19.2	1.4	304.7	41.9
P1c	**M1**	60:750:1	3	>95	100:37	16.8	1.5	313.3	45.2
P1d	**M1**	60:375:1	3	>95	100:23	21.6	1.6	321.8	51.6
P1e	**M1**	60:188:1	3	>95	100:16	32.4	1.5	340.3	63.2
P2a	**M2**	60:3000:1	3	>95	100:82	20.9	1.8	277.8	16.7
P2b	**M2**	60:750:1	3	>95	100:39	N.D.[d]	N.D.[d]	288.6	28.8
P2c	**M2**	60:188:1	3	>95	100:24	N.D.[d]	N.D.[d]	302.3	32.7
P3a	**M3**	60:3000:1	12	40	100:74	7.2	1.5	295.3	97.0
P3b	**M3**	60:750:1	12	34	100:35	10.8	1.9	298.3	127.1
P3c	**M3**	60:188:1	12	56	100:16	8.4	2.1	345.5	164.5

[a]Monomer conversions of ONB monomers were determined by ^{1}H NMR analysis. [b]The incorporation ratios of ONB to DHP were determined by ^{1}H NMR analysis. [c]The molecular weight and polydispersity of copolymers were assessed by DMF-SEC with polystyrene standards. [d]Those polymers were insoluble in DMF for SEC characterization.

thermodynamically unfavorable. In this study, we systematically investigate the copolymerization behavior of DHP and various exo-oxanorbornene monomers (M1-M3) under standard ROMP conditions (**Figure 1**). It was observed that a large excess of DHP was required to achieve a high incorporation of DHP units in the copolymers. By varying the feed ratio of DHP to oxanorbornene monomers, we obtained a series of poly(enol ether)s with different degrees of DHP incorporation. Thermogravimetric analysis (TGA) revealed that the thermal stability of poly(enol ether)s gradually decreased as the incorporation of DHP increased. In addition, the resulting poly(enol ether)s exhibit highly tunable glass transition temperatures (T_g) ranging from 16 to 165 °C, which are governed by the copolymer composition and oxanorbornene structure. Degradation study further showed that all the poly(enol ether)s were capable of undergoing acid-promoted degradation, highlighting their potential as bio-renewable and stimuli-responsive polymer materials.

2. Experimental Section

2.1. Materials. Furan (99%), maleic anhydride (99%), ethyl vinyl ether (98%), sulfuric acid (95-98%), anhydrous methanol (99.9%), anhydrous ethanol (99.5%),

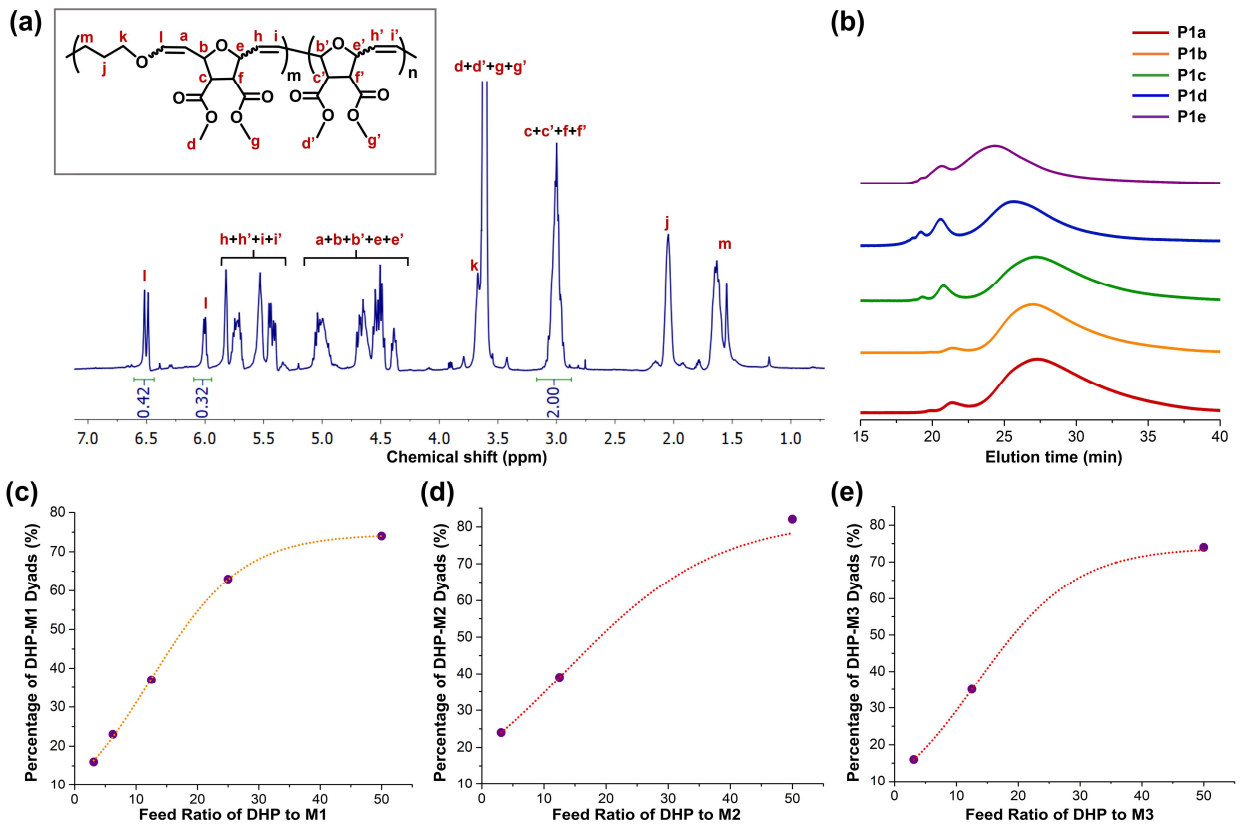

Figure 2. (a) ^{1}H NMR spectrum of P1a. The incorporation ratio of DHP to M1 was determined by comparing the signal integrations for enol ether vinyl protons (l) and M1 methine protons (c, c', f, f'). (b) SEC traces of P1-series copolymers. (c) Incorporation percentage of DHP as a function of the feed ratio of DHP to M1. (d) Incorporation percentage of DHP as a function of the feed ratio of DHP to M2. (e) Incorporation percentage of DHP as a function of the feed ratio of DHP to M3.

tetrahydrofuran (THF, 99%), and dichloromethane (DCM, 99%) were purchased from Fisher Scientific and used without purification. 3,4-Dihydropyran (DHP, 97%), methylamine (2.0 M in methanol) and Grubbs second generation catalyst (G2) were purchased from Sigma Aldrich and used as received. Oxanorbornene monomers (M1-M3) were synthesized according to our previous study.[33]

2.2. Computational Study. The ring strain energy of DHP was calculated by density functional theory (DFT) using Spartan software. Geometry optimizations and energy calculations were performed at the B3LYP/6-31 g(d) level of theory. The change of enthalpy or heat of formation (ΔH) was estimated as the enthalpy difference between the enthalpy of the ring-opened DHP and the total enthalpy of the isolated reactants (DHP + ethylene).

2.3. Instruments. ^{1}H NMR spectra were recorded on a Bruker spectrometer (400 MHz) in $CDCl_3$. Chemical shifts are given in ppm downfield from tetramethylsilane (TMS). The molecular weights of synthetic polymers and their degradation products were examined by a size exclusion chromatography (SEC) system (TOSOH EcoSEC HLC-8320) equipped with a set of Phenomenex Phenogel 5μ, 1K-75K, 300 x 7.80 mm in series with a Phenomex Phenogel 5μ, 10K-1000K, 300 x 7.80 mm columns following a guard column and two detectors including a RI detector and a UV detector. The measurements were performed using HPLC-grade DMF as the eluent at a flow rate of 0.5 mL/min at 35 °C and a series of polystyrene standards for the calibration of the columns. Differential scanning calorimetry (DSC) measurements were performed using a Guangdong Newgoer DSC-300C system under a nitrogen gas flow (100 mL/min). Two thermal cycles (-20 to 200 °C) with heating and cooling rates of 10 °C/min were performed. Glass transition temperatures were obtained from the second heating scan after removing the thermal history of polymers. Thermogravimetric analysis (TGA) was performed using a TA SDT Q600 system under a nitrogen gas flow (100 mL/min) with a heating rate of 10 °C/min. The temperature range for the analysis extended from ambient temperature to 650 °C.

2.4. Representative Synthesis of Poly(enol ether)s. In a typical procedure for the synthesis of P1a, M1 (95.5 mg, 0.47 mmol, 60 equiv.) and DHP (2.05 mL, 3000 equiv.) were dissolved in THF (1.5 mL) and then degassed by argon. Separately, a solution containing catalyst G2 (6.4 mg, 0.0075 mmol, 1.0 equiv.) and degassed THF (0.5 mL) was prepared, and then quickly added to

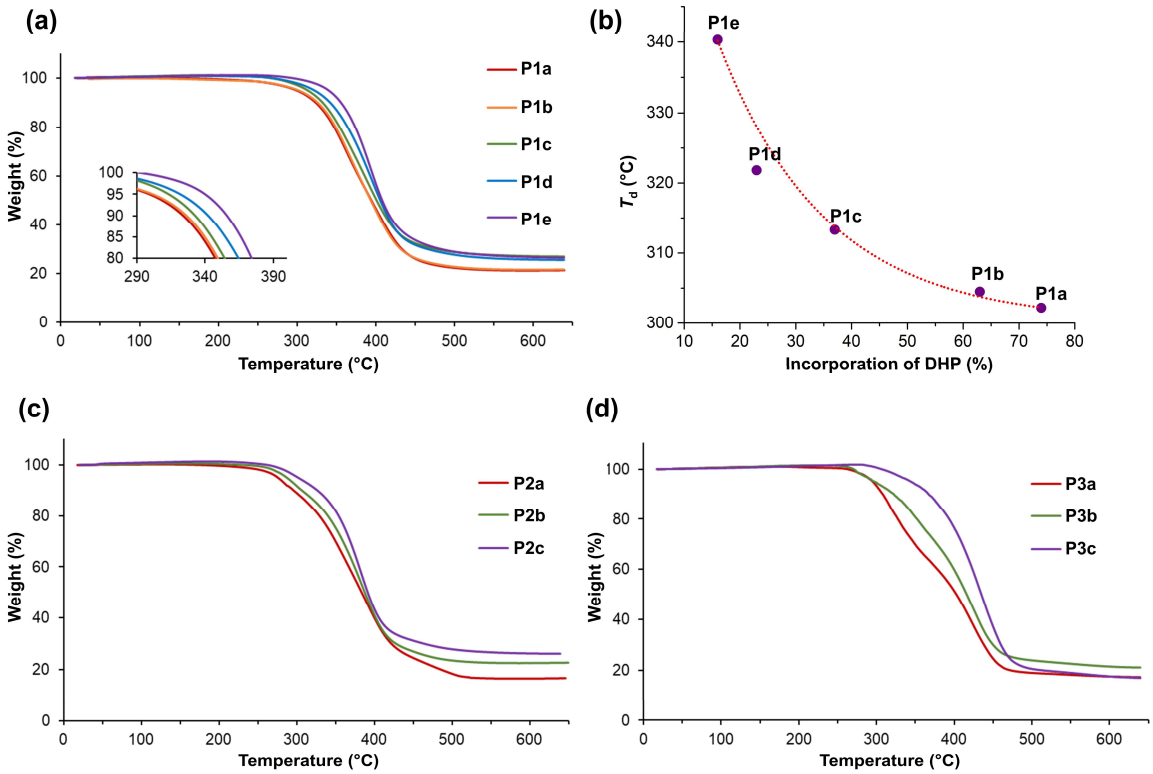

Figure 3. (a) TGA thermograms of P1 copolymers. (b) Decomposition temperature of P1 copolymers as a function of DHP incorporation. (c) TGA thermograms of P2 copolymers. (d) TGA thermograms of P3 copolymers.

the monomer solution. The reaction mixture was stirred for 3 h at room temperature. The polymerization was quenched with excess ethyl vinyl ether (80 μL, 0.85 mmol, 110 equiv.) and precipitated into cold methanol to obtain P1a.

2.5. Acid-Promoted Degradation of Poly(enol ether)s. In a typical protocol for polymer degradation, 20 μL of 1 M HCl aqueous solution was added into 980 μL of polymer solution in DMF (10 mg/mL). The resulting solution was analyzed using DMF-SEC at specified time intervals.

3. Results and Discussion

3.1. ROMP Synthesis of Poly(enol ether)s. We began our study by evaluating the ROMP reactivity of DHP monomer. According to DFT calculation, DHP has a RSE of 0.15 kcal/mol which is even smaller than that of cyclohexene (0.92 kcal/mol[40]) (**Figure S1**). In light of this, we reasoned that ring-opening of DHP would be thermodynamically disfavored under normal ROMP conditions. The computational analysis is in good agreement with our previous work which showed that DHP did not undergo bulk polymerization using Grubbs second generation catalyst (G2) at room temperature.[33]

While homopolymerization of DHP was not feasible, copolymerization of DHP with suitable comonomers would kinetically trap ring-opened DHP units in the propagating chains, leading to alternating dyads along the polymer backbone.[33, 36] Inspired by a recent work on the alternating ROMP of oxanorbornenes and cyclohexene,[41] we chose oxanorbornene derivatives as the comonomers to pair with DHP for the copolymerization study (**Figure 1**). It is worthy to mention that oxanorbornene monomers can be synthesized by the 100% atom economy Diels-Alder reaction between bio-derived furan and maleic anhydride, rendering the proposed DHP-oxanorbornene copolymers fully biomass-based.

In our previous study, we have demonstrated a proof-of-concept experiment on the copolymerization of M1 and DHP in the presence of G2.[33] Harnessing the same protocol, we resynthesized P1a that showed a similar molecular weight and DHP incorporation compared to the one reported by our previous work.[33] A library of copolymers of M1 and DHP was further prepared (**Table 1, P1a-P1e**). Considering the low ROMP reactivity of DHP, a large excess of DHP was used to enhance the incorporation of DHP units in the copolymers. A series of feed ratios of DHP to M1 was explored to target various compositions of copolymers. In all cases, high conversion (> 95%) of M1 was observed after three hours. As the feed ratio of DHP to M1 increased from 188:60 to 3000:60, the incorporation ratio of DHP to M1 increased from 16:100 to 74:100 in the resulting P1 copolymers (**Figures 2a, 2c and S2**). Notably, the ratio of M1 to G2 was set to 60:1 for all the P1 copolymers, achieving copolymers with similar molecular weights ranging from 16.8 to 32.4 kDa (**Figure 2b and Table 1, P1a-P1e**). The high molecular weight shoulders and broad molecular weight

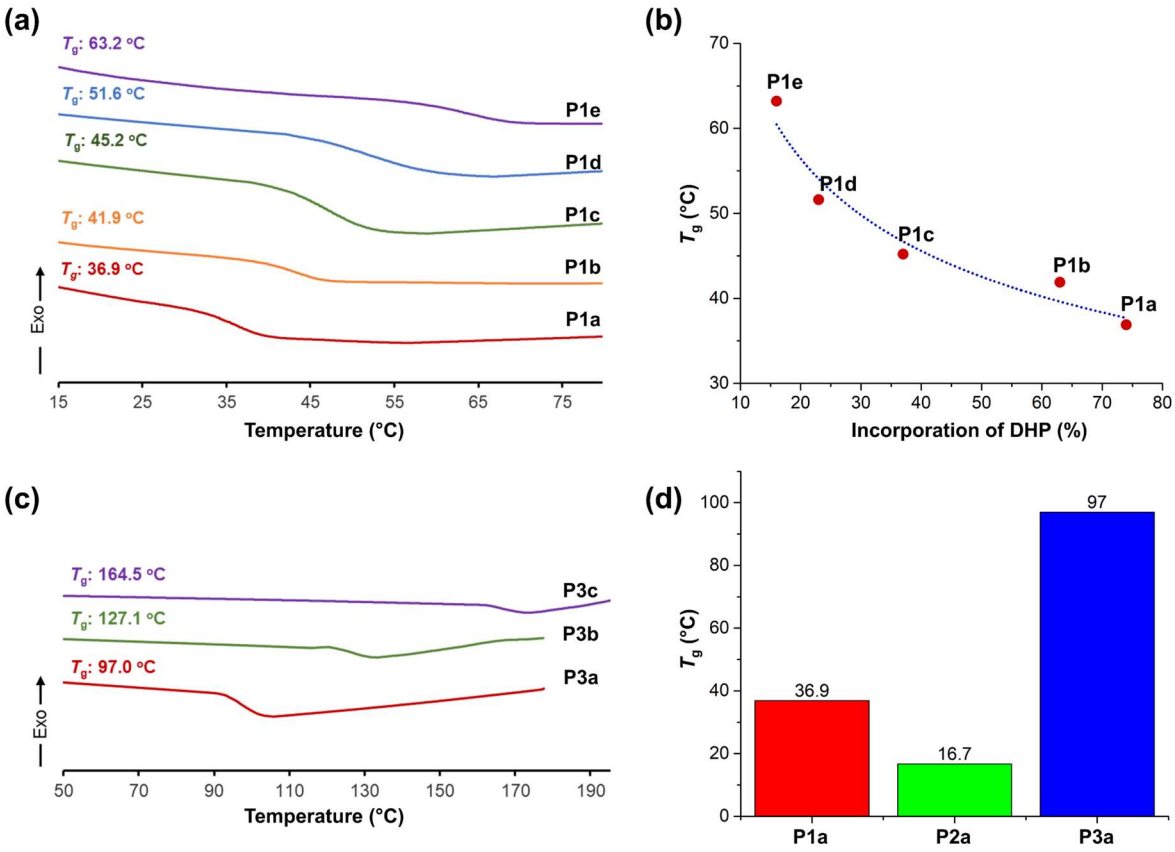

Figure 4. (a) DSC thermograms of P1 copolymers. T_g values were determined by the midpoint of the sigmoidal change in the heat capacity. (b) Glass transition temperature of P1 copolymers as a function of DHP incorporation. (c) DSC thermograms of P3 copolymers. (d) Glass transition temperatures of P1a, P2a, and P3a.

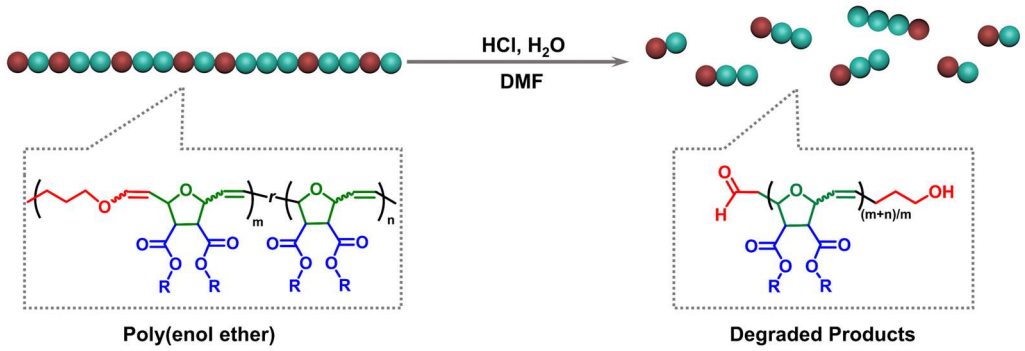

Figure 5. Schematic illustration of acid-promoted degradation of poly(enol ether)s based on DHP and oxanorbornenes.

distributions ($Đ$ = 1.4-1.6) of P1 copolymers can be attributed to the competing secondary metathesis or chain transfer reactions, which are common for less hindered polyolefin backbones.[42]

Compared with the DHF-M1 copolymers developed in our previous work,[33] the DHP-M1 copolymers have broader molecular weight distributions, suggesting a relatively poorer control over the polymerization. Moreover, a large excess of DHP monomers was required to achieve a high DHP incorporation into the copolymer, confirming its significantly lower ROMP reactivity than that of DHF.

To assess the versatility of this synthetic approach, two other oxanorbornene monomers including M2 and M3 were copolymerized with DHP, generating a library of P2 and P3 copolymers with different compositions (**Table 1, P2a-P2c and P3a-P3c**). Similar to P1 copolymers, the DHP incorporation in P2 and P3 copolymers gradually increased with an increasing feed ratio of DHP to M2 or M3 (**Figures 2d, 2e, and S3-S4**). A near quantitative conversion of M2 was achieved in the synthesis of P2-series copolymers. However, the copolymerization of DHP and imide-bearing M3 monomer was characterized with relatively low monomer conversions (34-56%) after 12 h,

resulting in P3 copolymers with low molecular weights (7.2-10.8 kDa) and broad molecular weight distributions (**Figure S5**). This can be attributed to the inherent low ROMP reactivity of imide-functional oxanorbornenes as described in a previous study.[34]

3.2. Thermal Properties of Poly(enol ether)s. To evaluate the industrial potential of as-synthesized polymer materials, we further investigated their thermal properties. Thermogravimetric analysis (TGA) was employed to determine the thermal stability of copolymers including P1-P3 (**Table 1 and Figure 3**). As shown in TGA thermograms, all the copolymers exhibited high decomposition temperatures (T_d at 5% weight loss) of at least 275 °C, demonstrating their excellent thermal stability. In the case of P1 series, the decomposition temperature gradually decreased from 340.3 to 302.2 °C as the incorporation ratio of DHP to M1 increased (**Figure 3a and 3b**). This result suggests that the incorporation of enol ether groups in the polyolefin backbone would reduce the thermal stability of copolymers. Nevertheless, the T_d of P1 copolymers remains above 300 °C even at the highest incorporation ratio of DHP to M1 (74:100). A

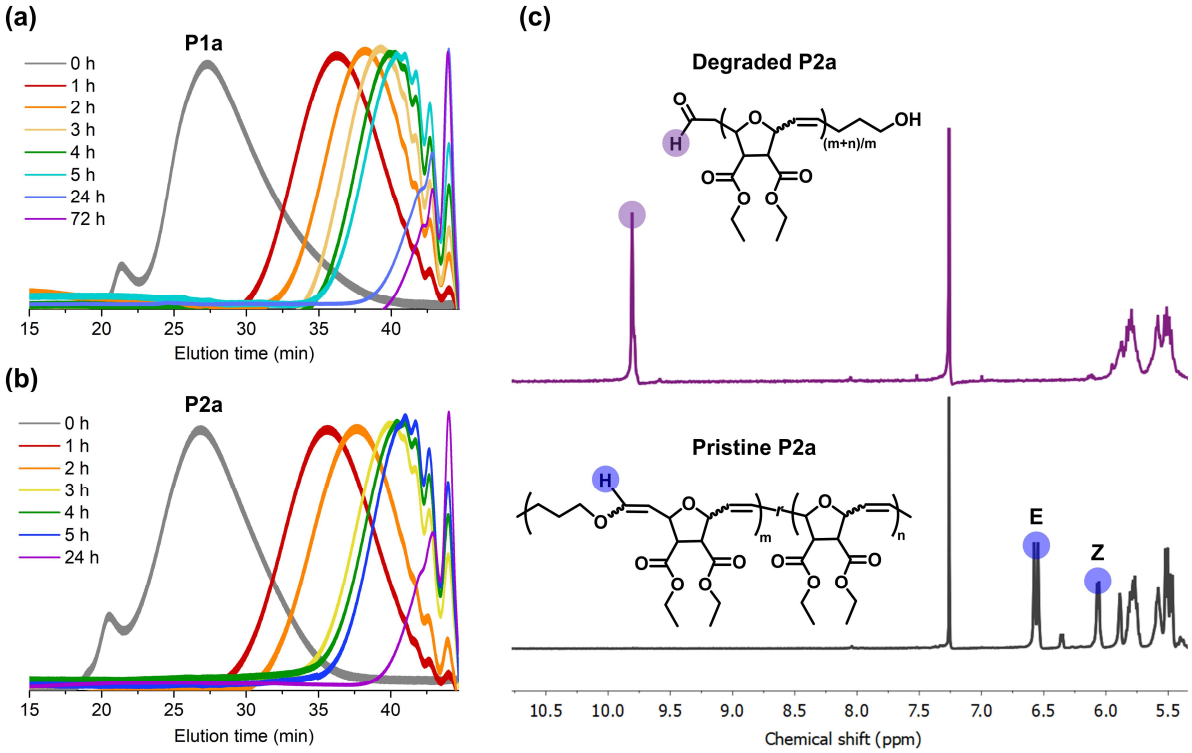

Figure 6. (a) SEC traces of P1a as a function of degradation time. The concentrations of HCl and water in DMF are 0.02 and 1.1 M, respectively. (b) SEC traces of P2a as a function of degradation time. The concentrations of HCl and water in DMF are 0.02 and 1.1 M, respectively. (c) ^{1}H NMR spectra of pristine P2a and fully degraded P2a.

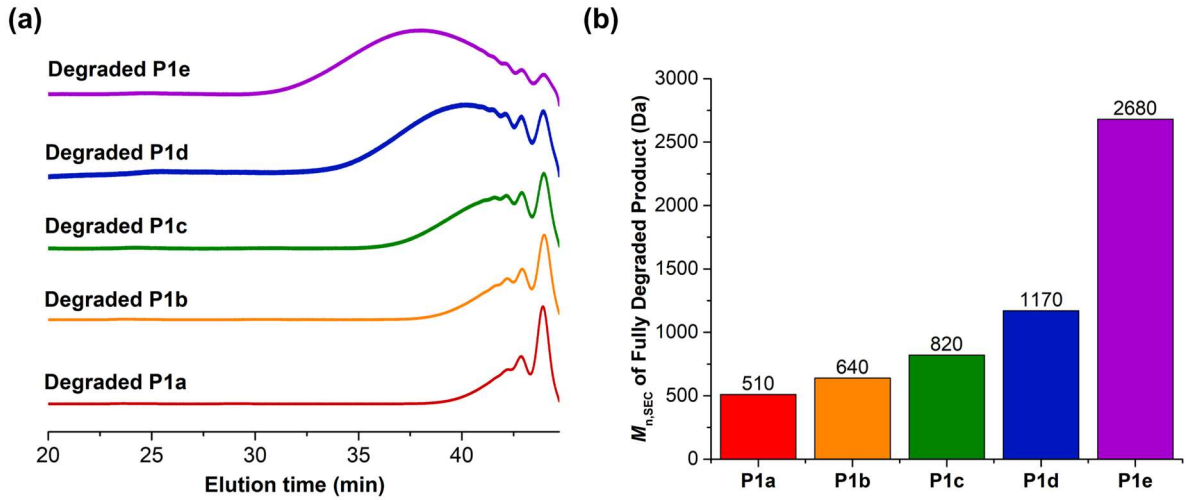

Figure 7. (a) SEC traces of final degradation products for P1a, P1b, P1c, P1d, and P1e. (b) The number-average molecular weights of degraded products for P1-series copolymers.

similar relationship between the T_d and DHP incorporation was also observed in P2 and P3 copolymers (**Figures 3c, 3d, and S6-S7**).

Differential scanning calorimetry (DSC) further revealed the glass-transition temperatures (T_g) of poly(enol ether)s (**Figure 4**). It was observed that the composition of copolymers played an important role in their T_g. As the incorporation of DHP increased, the glass transition temperature of copolymers decreased (**Figures 4a-4c and S8-S9**). This phenomenon can be attributed to the more flexible structure of ring-opened DHP in comparison with that of ring-opened oxanorbornenes. Moreover, the T_g values varied significantly by changing the side-chain functionalities on oxanorbornene monomers. Specifically, P2a bearing the flexible ethyl ester groups shows a T_g of 16.7 °C, which is markedly lower than that of P3a with a rigid imide structure (T_g = 97 °C) (**Figure 4d**). The ability to tune the glass transition temperatures in a wide range (16.7-165 °C) provides rich opportunities for the industrial applications of those copolymer materials from elastomers to plastics.

3.3. Acid-Triggered Degradation of Poly(enol ether)s. Poly(enol ether)s are recently emerging as a new class of degradable polymer materials due to the acid-sensitivity of enol ether repeating units.[32,43] We hypothesized that the DHP/ONB-based poly(enol ether)s developed in this study, upon treatment with acid, would be able to hydrolyze into bifunctional fragments with aldehyde and hydroxyl end groups (**Figure 5**). To examine the acid-degradability of those copolymers, we designed a degradation study that used HCl and water to promote the polymer hydrolysis in organic phase (i.e., DMF). SEC was employed to monitor the molecular weights of polymers through the degradation study. As shown in SEC analysis of P1-P3, the molecular weight of poly(enol ether)s gradually decreased as a function of degradation time, leading to small-sized molecules and oligomers after 24 h (**Figures 6a, 6b, and S10-S14**). Furthermore, NMR spectroscopy confirmed the completion of polymer degradation by showing the disappearance of enol ether vinyl proton signal (highlighted in blue), and the appearance of aldehyde protons (highlighted in purple) (**Figure 6c**).

Finally, we investigated the role of copolymer composition in tuning their degradability in terms of the size of final degradation products. Since DHP units are uniformly distributed along the copolymer backbone as DHP-oxanorbornene alternating dyads, we reasoned that a higher incorporation of acid-labile DHP units in the copolymer structure would lead to a higher degree of hydrolysis, producing smaller degradation products. Indeed, the number-average molecular weight of final degradation products decreased from 2,680 to 510 Da as the incorporation of DHP increased from 16% in P1e, to 74% in P1a (**Figure 7 and Table 1**). It is noteworthy to mention that the size of final degradation products was below 1000 Da when the DHP incorporation was above 37%.

4. Conclusions

In summary, we have presented a versatile synthetic approach to biomass-derived and acid-degradable poly(enol ether)s by ring-opening metathesis copolymerization of DHP and oxanorbornene monomers. This approach is highly modular, allowing us to tune the thermal properties of copolymers by simply varying the DHP percentage and oxanorbornene structure. The resulting copolymers exhibit a high thermal stability (T_d > 275 °C) and a wide range of glass transition temperatures (16-165 °C). Moreover, the sizes of final degradation products are tunable by controlling the composition of copolymers. Because poly(enol ether)s are acid-sensitive, we envision that they can be potentially used for producing pH-responsive drug delivery systems that would release therapeutics in acidic environments such as tumors. Given the increasing trend in developing biomass-derived polymers for enhanced sustainability and reduced environmental impact, we envision that the bio-derived poly(enol ether)s developed in this work have substantial potential as a class of sustainable, low carbon-footprint, and degradable polymer materials.

ASSOCIATED CONTENT

Supporting Information. This material is available free of charge via the Internet at http://pubs.acs.org.

Synthetic procedures of polymers; DFT calculation of RSE of DHP; ^{1}H NMR analysis of P1, P2, and P3; DSC thermograms of P2-series copolymers; SEC traces of P3-series copolymers; SEC analysis of P1b, P1c, P1d, P1e, and P3b during the degradation study.

AUTHOR INFORMATION

Corresponding Author

Dr. Hao Sun, Email: hasun@newhaven.edu

Author Contributions

The manuscript was written through contributions of all authors. All authors have given approval to the final version of the manuscript.

ACKNOWLEDGMENT

This material is based upon work supported by a LEAPS-MPS award from the National Science Foundation under Grant No. [CHE-2316842].

REFERENCES

1. Wamba, S. F.; Fotso, M.; Mosconi, E.; Chai, J., Assessing the potential of plastic waste management in the circular economy: a longitudinal case study in an emerging economy. *Ann. Oper. Res.* **2023**, 1-23.

2. Sun, H.; Kabb, C. P.; Sims, M. B.; Sumerlin, B. S., Architecture-transformable polymers: Reshaping the future of stimuli-responsive polymers. *Prog. Polym. Sci.* **2019,** *89*, 61-75.

3. Ma, T.; Easley, A. D.; Thakur, R. M.; Mohanty, K. T.; Wang, C.; Lutkenhaus, J. L., Nonconjugated Redox-Active Polymers: Electron Transfer Mechanisms, Energy Storage, and Chemical Versatility. *Annu. Rev. Chem. Biomol. Eng.* **2023,** *14*, 187-216.

4. Zhu, Y.; Romain, C.; Williams, C. K., Sustainable polymers from renewable resources. *Nature* **2016,** *540* (7633), 354-362.

5. Atiwesh, G.; Mikhael, A.; Parrish, C. C.; Banoub, J.; Le, T. T., Environmental impact of bioplastic use: A review. *Heliyon* **2021,** *7* (9), e07918.

6. Wang, Z.; Ganewatta, M. S.; Tang, C., Sustainable polymers from biomass: Bridging chemistry with materials and processing. *Prog. Polym. Sci.* **2020,** *101*, 101197.

7. Popp, J.; Kovacs, S.; Olah, J.; Diveki, Z.; Balazs, E., Bioeconomy: Biomass and biomass-based energy supply and demand. *N. Biotechnol.* **2021,** *60*, 76-84.

8. Rosenboom, J. G.; Langer, R.; Traverso, G., Bioplastics for a circular economy. *Nat. Rev. Mater.* **2022,** *7* (2), 117-137.

9. Yao, K.; Tang, C., Controlled Polymerization of Next-Generation Renewable Monomers and Beyond. *Macromolecules* **2013,** *46* (5), 1689-1712.

10. Palà, M.; Woods, S. E.; Hatton, F. L.; Lligadas, G., RDRP (Meth)acrylic Homo and Block Polymers from Lignocellulosic Sugar Derivatives. *Macromol. Chem. Phys.* **2022,** *223* (13), 2200005.

11. Parkatzidis, K.; Boner, S.; Wang, H. S.; Anastasaki, A., Photoinduced Iron-Catalyzed ATRP of Renewable Monomers in Low-Toxicity Solvents: A Greener Approach. *ACS Macro Lett.* **2022,** *11* (7), 841-846.

12. Wang, J.; Yuan, L.; Wang, Z.; Rahman, M. A.; Huang, Y.; Zhu, T.; Wang, R.; Cheng, J.; Wang, C.; Chu, F.; Tang, C., Photoinduced Metal-Free Atom Transfer Radical Polymerization of Biomass-Based Monomers. *Macromolecules* **2016,** *49* (20), 7709-7717.

13. Hatton, F. L., Recent advances in RAFT polymerization of monomers derived from renewable resources. *Polym. Chem.* **2020,** *11* (2), 220-229.

14. Porwal, M. K.; Reddi, Y.; Saxon, D. J.; Cramer, C. J.; Ellison, C. J.; Reineke, T. M., Stereoregular functionalized polysaccharides via cationic ring-opening polymerization of biomass-derived levoglucosan. *Chem. Sci.* **2022,** *13* (16), 4512-4522.

15. Wu, L.; Zhou, Z.; Sathe, D.; Zhou, J.; Dym, S.; Zhao, Z.; Wang, J.; Niu, J., Precision native polysaccharides from living polymerization of anhydrosugars. *Nat. Chem.* **2023,** *15*, 1276-1284.

16. Debsharma, T.; Yagci, Y.; Schlaad, H., Cellulose-Derived Functional Polyacetal by Cationic Ring-Opening Polymerization of Levoglucosenyl Methyl Ether. *Angew. Chem. Int. Ed.* **2019,** *58* (51), 18492-18495.

17. Porwal, M. K.; Ellison, C. J.; Reineke, T. M., Biobased Copolymers via Cationic Ring-Opening Copolymerization of Levoglucosan Derivatives and epsilon-Caprolactone. *ACS Macro Lett.* **2023,** *12* (7), 935-942.

18. Strick, B. F.; Delferro, M.; Geiger, F. M.; Thomson, R. J., Investigations into Apopinene as a Biorenewable Monomer for Ring-Opening Metathesis Polymerization. *ACS Sustain. Chem. Eng.* **2015,** *3* (7), 1278-1281.

19. Engelen, S.; Droesbeke, M.; Aksakal, R.; Du Prez, F. E., Ring-Opening Metathesis Polymerization for the Synthesis of Terpenoid-Based Pressure-Sensitive Adhesives. *ACS Macro Lett.* **2022,** *11* (12), 1378-1383.

20. Yarolimek, M. R.; Bookbinder, H. R.; Coia, B. M.; Kennemur, J. G., Ring-Opening Metathesis Polymerization of delta-Pinene: Well-Defined Polyolefins from Pine Sap. *ACS Macro Lett.* **2021,** *10* (6), 760-766.

21. Yarolimek, M. R.; Coia, B. M.; Bookbinder, H. R.; Kennemur, J. G., Investigating the effect of α-pinene on the ROMP of δ-pinene. *Polym. Chem.* **2021,** *12*, 5048-5058.

22. Ganewatta, M. S.; Ding, W.; Rahman, M. A.; Yuan, L.; Wang, Z.; Hamidi, N.; Robertson, M. L.; Tang, C., Biobased Plastics and Elastomers from Renewable Rosin via "Living" Ring-Opening Metathesis Polymerization. *Macromolecules* **2016,** *49* (19), 7155-7164.

23. Hu, Y.; Ran, Q.; Wei, S.; Wang, C.; Wu, Z.; Xu, E.; Luo, Z.; Jia, P.; Sha, Y., Closed-loop recycling of lignin-based sustainable polymers with an all-hydrocarbon backbone. *Green Chem.* **2023,** *25* (15), 5858-5864.

24. Feng, Y.; Jie, S.; Li, B.-G., Synthesis of ethylene/vinyl ester copolymers with pendent linear branches via ring-opening metathesis polymerization of fatty acid-derived cyclooctenes. *J. Polym. Sci. Part A: Polym. Chem.* **2017,** *55* (13), 2211-2220.

25. Fadlallah, S.; Peru, A.; Flourat, A. L.; Allais, F., A straightforward access to functionalizable polymersthrough ring-opening metathesis polymerization oflevoglucosenone-derived monomers. *Eur. Polym. J.* **2020,** *138*, 109980.

26. Bai, Y.; Clark, J. H.; Farmer, T. J.; Ingram, I. D. V.; North, M., Wholly biomass derivable sustainable polymers by ring-opening metathesis polymerisation of monomers obtained from furfuryl alcohol and itaconic anhydride. *Polym. Chem.* **2017,** *8* (20), 3074-3081.

27. Diot-Neant, F.; Migeot, L.; Hollande, L.; Reano, F. A.; Domenek, S.; Allais, F., Biocatalytic Synthesis and Polymerization via ROMP of New Biobased Phenolic Monomers: A Greener Process toward Sustainable Antioxidant Polymers. *Front Chem.* **2017,** *5*, 126.

28. Naguib, M.; Yassin, M. A., Polymeric Antioxidant via ROMP of Bioderived Tricyclic Oxanorbornene Based on Vanillin and Furfurylamine. *ACS Appl. Mater. Interfaces* **2022,** *4* (3), 2181-2188.

29. Debsharma, T.; Behrendt, F. N.; Laschewsky, A.; Schlaad, H., Ring-opening metathesis polymerization of biomass-derived levoglucosenol. *Angew. Chem. Int. Ed.* **2019,** *58*, 6718-6721.

30. Bhaumik, A.; Peterson, G. I.; Kang, C.; Choi, T. L., Controlled Living Cascade Polymerization To Make Fully Degradable Sugar-Based Polymers from D-Glucose and D-Galactose. *J. Am. Chem. Soc.* **2019,** *141* (31), 12207-12211.

31. Leitgeb, A.; Wappel, J.; Slugovc, C., The ROMP toolbox upgraded. *Polymer* **2010,** *51* (14), 2927-2946.

32. Feist, J. D.; Xia, Y., Enol Ethers Are Effective Monomers for Ring-Opening Metathesis Polymerization: Synthesis of Degradable and Depolymerizable Poly(2,3-dihydrofuran). *J. Am. Chem. Soc.* **2020,** *142* (3), 1186-1189.

33. Sun, H.; Ibrahim, T.; Ritacco, A.; Durkee, K., Biomass-Derived Degradable Polymers via Alternating Ring-Opening Metathesis Polymerization of Exo-Oxanorbornenes and Cyclic Enol Ethers. *ACS Macro Lett.* **2023,** *12* (12), 1642–1647.

34. An, T.; Ryu, H.; Choi, T. L., Living Alternating Ring-Opening Metathesis Copolymerization of 2,3-Dihydrofuran to Provide Completely Degradable Polymers. *Angew. Chem. Int. Ed.* **2023,** *62* (47), e202309632.

35. Feist, J. D.; Lee, D. C.; Xia, Y., A versatile approach for the synthesis of degradable polymers via controlled ring-opening metathesis copolymerization. *Nat. Chem.* **2022,** *14* (1), 53-58.

36. Sui, X.; Zhang, T.; Pabarue, A. B.; Fu, L.; Gutekunst, W. R., Alternating Cascade Metathesis Polymerization of Enynes and Cyclic Enol Ethers with Active Ruthenium Fischer Carbenes. *J. Am. Chem. Soc.* **2020,** *142* (30), 12942-12947.

37. Sui, X.; Gutekunst, W. R., Cascade Alternating Metathesis Cyclopolymerization of Diynes and Dihydrofuran. *ACS Macro Lett.* **2022,** *11* (5), 630-635.

38. Tashiro, K.; Akiyama, M.; Kashiwagi, K.; Okazoe, T., The Fluorocarbene Exploit: Enforcing Alternation in Ring-Opening Metathesis Polymerization. *J. Am. Chem. Soc.* **2023,** *145* (5), 2941-2950.

39. Li, X.; Tian, J.; Liu, H.; Hu, X.; Zhang, J.; Xia, C.; Chen, J.; Liu, H.; Huang, Z., Efficient Synthesis of 5-Amino-1-pentanol from Biomass-Derived Dihydropyran over Hydrotalcite-Based Ni–Mg3AlOx Catalysts. *ACS Sustain. Chem. Eng.* **2020,** *8* (16), 6352-6362.

40. Choi, K.; Hong, S. H., Chemically recyclable oxygen-protective polymers developed by ring-opening metathesis homopolymerization of cyclohexene derivatives. *Chem* **2023,** *9* (9), 2637-2654.

41. Pal, S.; Alizadeh, M.; Kong, P.; Kilbinger, A. F. M., Oxanorbornenes: promising new single addition monomers for the metathesis polymerization. *Chem. Sci.* **2021,** *12* (19), 6705-6711.

42. Walker, R.; Conrad, R. M.; Grubbs, R. H., The Living ROMP of trans-Cyclooctene. *Macromolecules* **2009**, 42, 599-605.

43. Shimomoto, H.; Mori, T.; Itoh, T.; Ihara, E., Poly(β-keto enol ether) Prepared by Three-Component Polycondensation of Bis(diazoketone), Bis(1,3-diketone), and Tetrahydrofuran: Mild Acid-Degradable Polymers To Afford Well-Defined Low Molecular Weight Components. *Macromolecules* **2019,** *52* (15), 5761-5768.

Insert Table of Contents artwork here